# Low-lying excited states of the odd-proton nuclei with $Z \approx 100$

N. Yu. Shirikova,* A. V. Sushkov,† and R. V. Jolos‡
*Joint Institute for Nuclear Research, 141980 Dubna, Russia*

(Received 30 September 2013; revised manuscript received 15 November 2013; published 17 December 2013)

**Background:** Theoretical investigations of the structure of the low-lying states of nuclei with $Z \approx 100$ play an important role in understanding the properties of nuclei belonging to the new region of the nuclide chart which is available now for experimental study.
**Purpose:** We perform the calculations of the excitation energies and wave functions of the low-lying states of nuclei with $Z \approx 100$.
**Methods:** The quasiparticle-phonon model, which takes into account an interaction of the quasiparticles and phonons of different multipolarities, is used as a basis for the calculations.
**Results:** The excitation energies and the quasiparticle-phonon structure of the low-lying states with excitation energies up to 1200 keV of the odd-proton nuclei $^{239-251}$Bk, $^{243-255}$Es, $^{247-257}$Md, $^{253,255}$Lr, and $^{261,263}$Db are calculated.
**Conclusions:** It is shown that starting from 600 keV the excitation of the phonons and the quasiparticle-phonon interaction play an important role in the description of the properties of the excited states of nuclei with $Z \approx 100$.

DOI: 10.1103/PhysRevC.88.064319 PACS number(s): 21.10.Re

## I. INTRODUCTION

The experimental investigations of the structure of very heavy nuclei are in need of theoretical support to help analyze the experimental data. Calculations of the single-quasiparticle spectra of very heavy nuclei with $Z \approx 100$ have been performed by several authors [1, 2]. But in the majority of the theoretical papers the quasiparticle-phonon coupling, i.e., the effect of the fluctuations of the nuclear mean field, was not taken into account (see, however, [3]). Nevertheless, it is known from the investigations of the properties of the rare-earth nuclei and actinides [4] that the quasiparticle-phonon interaction can strongly influence the excitation spectra of well deformed nuclei at excitation energies even below 1 MeV. The other important effect specific for the odd nuclei is the blocking effect [4], which can influence the superfluid pair correlations of nucleons. It is the aim of the present paper to describe the properties of the low-lying states of the odd-proton nuclei with $Z \approx 100$, taking into account both the quasiparticle-phonon interaction and the blocking effect.

## II. QUASIPARTICLE-PHONON MODEL

The Hamiltonian of the quasiparticle-phonon model [4] contains the mean field part for protons and neutrons, the monopole pairing interaction, and the multipole-multipole interaction acting in the particle-hole and the particle-particle channels:

$$H = H_{sp} + V_{\text{pair}} + V_M^{ph} + V_M^{pp}. \quad (1)$$

Here $H_{sp}$ is a one-body Hamiltonian, $V_{\text{pair}}$ describes the monopole pairing, and $V_M^{ph}$ and $V_M^{pp}$ are the particle-hole separable multipole interaction and particle-particle multipole pairing interaction, respectively.

For the mean field term we have taken the Woods–Saxon potential

$$\begin{aligned} V_{sp}(\vec{r}) &= V_{WS}(\vec{r}) + V_{so}(\vec{r}), \\ V_{WS}(\vec{r}) &= -V_0(1+\exp[\{r - R(\theta,\varphi)\}/a])^{-1}, \\ V_{so}(\vec{r}) &= -\kappa(\vec{p}\times\sigma)\nabla V_{WS}(\vec{r}), \end{aligned} \quad (2)$$

with the parameters taken from [5]. The parameters of the Woods-Saxon potential are fixed so that after taking into account the quasiparticle-phonon interaction we get a correct description of the energies of the states of odd nuclei whose structure is dominated by the one-quasiparticle components (see [4], page 145, last paragraph, and [5]). Thus the double counting of the quasiparticle-phonon interaction is avoided in our calculations. These parameters are quite close to those used in the calculations for the rare-earth nuclei [5–7].

In recent years many calculations of the self-consistent nuclear mean field, based on different choices of the energy-density functional, have been performed [8–11]. In contrast to them the nuclear mean field potential used in the quasiparticle-phonon model is not self-consistent. There are, however, some arguments which justify an application of the Woods-Saxon potential as an approximation to the nuclear mean field potential for deformed nuclei with $Z = 97$–105. In the heavier nuclei in which single-particle states with larger orbital momenta $l$ are occupied, a possible appearance of a dip at the center of the nuclear mean field potential should be taken into account.

The experimentally investigated nuclei with $Z \approx 100$ are deformed [12–14]. Beautiful experimental confirmation of the quadrupole deformation of the heavy elements with $Z \approx 100$ comes from $\gamma$–ray spectroscopy around $Z = 102$ and $N = 152$; namely, the identification of the rotational bands in $^{254}$No and its neighbors. The deformation leads to a more equal distribution of the single-particle states emerging from the

*shirikov@theor.jinr.ru
†sushkov@theor.jinr.ru
‡jolos@theor.jinr.ru

 

TABLE I. Calculated excitation energies $E^*_{\rm cal}$ and the structure of the excited states of $^{239}$Bk. The energies are given in keV. $Q_{\lambda\mu}$ denotes a phonon of multipolarity $\lambda\mu$ and $i = 1$.

| $J^\pi$ | $E^*_{\rm cal}$ | Structure |
|---|---|---|
| $7/2^+$ | 0 | $7/2[633]$ 79% + $7/2[633] \times Q_{20}$ 14% |
| $3/2^-$ | 166 | $3/2[521]$ 85% |
| $1/2^+$ | 431 | $1/2[660]$ 64% + $3/2[651]\times Q_{22}$ 28% |
| $3/2^+$ | 546 | $3/2[651]$ 46% + $1/2[660]\times Q_{22}$ 49% |
| $1/2^-$ | 605 | $3/2[521]\times Q_{22}$ 69% + $1/2[521]$ 23% |
| $5/2^-$ | 646 | $5/2[523]$ 85% + $5/2[523]\times Q_{20}$ 6% |
| $5/2^+$ | 690 | $5/2[642]$ 76% |
| $3/2^+$ | 806 | $7/2[633]\times Q_{22}$ 95% |
| $7/2^-$ | 875 | $3/2[521]\times Q_{22}$ 100% |
| $5/2^+$ | 893 | $1/2[660]\times Q_{22}$ 86% + $5/2[402]$ 11% |
| $5/2^-$ | 939 | $5/2[512]$ 30% + $7/2[633]\times Q_{31}$ 61% |
| $1/2^-$ | 946 | $1/2[530]$ 71% + $5/2[642]\times Q_{32}$ 12% |
| $9/2^-$ | 961 | $5/2[523]\times Q_{22}$ 100% |
| $1/2^+$ | 1010 | $5/2[642]\times Q_{22}$ 75% + $1/2[400]$ 13% |
| $3/2^-$ | 1099 | $3/2[521]\times Q_{20}$ 95% |
| $7/2^-$ | 1135 | $7/2[514]$ 78% + $7/2[633]\times Q_{30}$ 15% |
| $9/2^+$ | 1157 | $5/2[642]\times Q_{22}$ 65% + $9/2[624]$ 30% |
| $9/2^-$ | 1192 | $7/2[633]\times Q_{31}$ 97% |
| $7/2^+$ | 1241 | $7/2[633]\times Q_{20}$ 81% +$7/2[633]$ 9%+$3/2[521]\times Q_{32}$ 8% |
| $9/2^+$ | 1297 | $9/2[624]$ 55% + $5/2[642]\times Q_{22}$ 35% |

high-$j$ (for these states the maximum of the single-particle wave function is shifted closer to the nuclear surface) and low-$j$ spherical subshells. For this reason a density profile of a deformed nucleus is relatively flat inside the nucleus [15–17]. This resembles the use of the phenomenological Woods-Saxon potential for these nuclei.

A comparison of the results of the self-consistent calculations with the single-particle spectra obtained with the Woods-Saxon potential demonstrates a very good agreement both for protons and neutrons [18]. The large gaps in the single-particle spectra for neutrons at $N = 152$ and protons at $Z = 96$ and 100 are clearly seen. The results obtained in [19] and [20] indicate the existence of the proton $1/2^-[521]$ and $7/2^-[514]$ single-particle states near the Fermi level at $Z = 103$ in agreement with our scheme.

TABLE II. Experimental $E^*_{\rm exp}$ and calculated $E^*_{\rm cal}$ excitation energies and the structure of the excited states of $^{243}$Bk. The energies are given in keV. The experimental data are taken from [32]. $Q_{\lambda\mu}$ denotes a phonon of multipolarity $\lambda\mu$ and $i = 1$. We indicate the cases when phonons with $i = 2$ contribute to the structure of the excited state.

| $J^\pi$ | $E^*_{\rm exp}$ | $E^*_{\rm cal}$ | Structure |
|---|---|---|---|
| $7/2^+$ | 46 | 0 | $7/2[633]$ 93% |
| $3/2^-$ | 0 | 25 | $3/2[521]$ 94% |
| $5/2^-$ | | 475 | $5/2[523]$ 96% |
| $1/2^+$ | | 625 | $1/2[660]$ 87% + $3/2[651]\times Q_{222}$ 7% |
| $5/2^+$ | | 634 | $5/2[642]$ 84% + $1/2[530]\times Q_{32}$ 8% |
| $1/2^-$ | | 826 | $1/2[530]$ 70% + $5/2[642]\times Q_{32}$ 20% |
| $3/2^+$ | | 828 | $3/2[651]$ 74% + $1/2[660]\times Q_{222}$ 14% |
| $5/2^-$ | | 984 | $5/2[512]$ 28% + $7/2[633]\times Q_{31}$ 63% |
| $7/2^-$ | | 1000 | $7/2[514]$ 78% + $7/2[633]\times Q_{30}$ 19% |
| $1/2^-$ | | 1057 | $1/2[521]$ 60% + $3/2[521]\times Q_{222}$ 34% |
| $9/2^+$ | | 1074 | $9/2[624]$ 88% + $5/2[512]\times Q_{32}$ 9% |
| $1/2^+$ | | 1114 | $3/2[521]\times Q_{32}$ 80% + $3/2[521]\times Q_{31}$ 8% + $5/2[523]\times Q_{32}$ 7% |
| $3/2^-$ | | 1150 | $7/2[633]\times Q_{32}$ 93% |
| $9/2^-$ | | 1157 | $7/2[633]\times Q_{31}$ 98% |
| $7/2^-$ | | 1164 | $3/2[521]\times Q_{22}$ 100% |
| $5/2^+$ | | 1174 | $3/2[521]\times Q_{31}$ 99% |
| $3/2^+$ | | 1180 | $3/2[402]$ 20% + $5/2[523]\times Q_{31}$ 20% + $3/2[521]\times Q_{30}$ 49% |
| $7/2^+$ | | 1192 | $3/2[521]\times Q_{32}$ 96% |
| $9/2^+$ | | 1231 | $5/2[523]\times Q_{32}$ 100% |

TABLE III. Experimental $E^*_{\rm exp}$ and calculated $E^*_{\rm cal}$ excitation energies and the structure of the excited states of $^{249}$Bk. The energies are given in keV. The experimental data are taken from [32]. $Q_{\lambda\mu}$ denotes a phonon of multipolarity $\lambda\mu$ and $i = 1$.

| $J^\pi$ | $E^*_{\rm exp}$ | $E^*_{\rm cal}$ | Structure |
|---|---|---|---|
| $7/2^+$ | 0 | 0 | 7/2[633] 94% |
| $3/2^-$ | 9 | 27 | 3/2[521] 95% |
| $5/2^-$ | | 396 | 5/2[523] 95% |
| $1/2^+$ | 378 | 457 | 1/2[660] 85% + 3/2[651]$\times Q_{22}$ 10% |
| $5/2^+$ | 389 | 470 | 5/2[642] 823% + 5/2[642]$\times Q_{20}$ 10% |
| $3/2^+$ | | 671 | 3/2[651] 75% + 1/2[660]$\times Q_{22}$ 20 % |
| $1/2^-$ | | 787 | 1/2[530] 79% + 5/2[642]$\times Q_{32}$ 12% |
| $7/2^-$ | | 879 | 7/2[514] 96% |
| $1/2^-$ | | 883 | 1/2[521] 52% + 3/2[521]$\times Q_{22}$ 43% |
| $9/2^+$ | | 955 | 9/2[624] 90% + 5/2[512]$\times Q_{32}$ 8% |
| $5/2^-$ | | 1094 | 5/2[512] 65% + 7/2[633]$\times Q_{31}$ 15% + 9/2[624]$\times Q_{32}$ 13% |
| $3/2^+$ | | 1126 | 3/2[402] 26% + 7/2[633]$\times Q_{22}$ 64% |
| $7/2^-$ | | 1216 | 3/2[521]$\times Q_{22}$ 100% |
| $1/2^+$ | | 1252 | 3/2[521]$\times Q_{32}$ 51% + 5/2[642]$\times Q_{22}$ 19% + 1/2[400] 14% + 5/2[523]$\times Q_{32}$ 12% |
| $5/2^+$ | | 1284 | 1/2[660]$\times Q_{22}$ 82% + 5/2[402] 14% |
| $3/2^-$ | | 1290 | 7/2[633]$\times Q_{32}$ 94% |

The analysis of the proton single-particle states [21] shows that the lowest states just above the gap at $Z = 96$ are $7/2^+[633]$ and $3/2^-[521]$ orbitals. The next three orbitals are $7/2^-[514]$, $1/2^-[521]$, and $9/2^+[624]$. This is just in correspondence with the level scheme calculated with the Woods-Saxon potential at the quadrupole deformation parameter $\beta_2 = 0.26$.

A comparison of the neutron single-particle level scheme of the Woods-Saxon potential with the single-particle energies extracted from the experimental data in [22] shows that in both cases just above $N = 152$ there are the same closely lying single-particle levels, namely, $7/2^+[613]$, $1/2^+[620]$, $3/2^+[622]$, and $11/2^-[725]$. There is, however, a small difference in the ordering of the first two levels. We mention, however, that in [22] the energies of the neutron single-particle levels have been extracted from the experimental data without taking into account the particle-vibration coupling.

TABLE IV. Experimental $E^*_{\rm exp}$ and calculated $E^*_{\rm cal}$ excitation energies and the structure of the excited states of $^{249}$Es. The energies are given in keV. The experimental data are taken from [32]. $Q_{\lambda\mu}$ denotes a phonon of multipolarity $\lambda\mu$ and $i = 1$.

| $J^\pi$ | $E^*_{\rm exp}$ | $E^*_{\rm cal}$ | Structure |
|---|---|---|---|
| $7/2^+$ | 0 | 0 | 7/2[633] 96% |
| $3/2^-$ | | 44 | 3/2[521] 97% |
| $9/2^+$ | | 504 | 9/2[624] 88% + 5/2[512]$\times Q_{32}$ 10% |
| $7/2^-$ | 353? | 516 | 7/2[514] 98% |
| $1/2^-$ | | 689 | 1/2[521] 91% + 3/2[521]$\times Q_{22}$ 6% |
| $5/2^-$ | | 723 | 5/2[512] 67% + 9/2[624]$\times Q_{32}$ 25% |
| $5/2^-$ | | 775 | 5/2[523] 95% |
| $5/2^+$ | | 865 | 5/2[642] 77% + 1/2[530]$\times Q_{32}$ 9% |
| $3/2^-$ | | 892 | 7/2[633]$\times Q_{32}$ 97% |
| $1/2^+$ | | 900 | 1/2[660] 83% + 3/2[651]$\times Q_{22}$ 8% |
| $1/2^+$ | | 924 | 3/2[521]$\times Q_{32}$ 98% |
| $7/2^+$ | | 952 | 3/2[521]$\times Q_{32}$ 100% |
| $1/2^-$ | | 1095 | 1/2[530] 62% + 5/2[642]$\times Q_{32}$ 26% |
| $3/2^+$ | | 1125 | 3/2[651] 76% + 1/2[660]$\times Q_{22}$ 17% |
| $9/2^-$ | | 1258 | 7/2[633]$\times Q_{31}$ 99% |
| $3/2^+$ | | 1287 | 3/2[402] 12% + 7/2[633]$\times Q_{22}$ 77% |
| $5/2^+$ | | 1293 | 3/2[521]$\times Q_{31}$ 95% |
| $7/2^-$ | | 1384 | 3/2[521]$\times Q_{22}$ 100% |

There is some experimental information about the quadrupole deformation parameter $\beta_2$. Although the lifetimes have not been measured, the $B(E2)$ values of rotors are related to the energies of the first $2^+$ levels by the empirical Grodzins relation [23]. Using this relation the value $\beta_2 = 0.27(2)$ has been deduced for $^{254}$No [24]. The recent calculations [25] give the value $\beta_2 = 0.26$ for nuclei with $Z = 96$–104 and $N = 148$–156. The results of calculations presented in [26] demonstrate a stability of the quadrupole deformation for nuclei with $Z = 100$–104. For these reasons we have used the same value of $\beta_2 = 0.26$ for all considered nuclei. A comparison of the single-particle energies of the levels lying around the Fermi surface and calculated for $\beta_2$=0.25 and $\beta_2 = 0.27$ with those obtained for $\beta_2 = 0.26$ shows that in many cases deviations are less than 100 keV, although for some states they take the values 150 keV or even 350 keV.

The values of the diffusion parameter used in our calculations have been fixed in the investigations of the properties of the actinide nuclei [5]. They are closed to the values used in [27] where $a = 0.70$ fm for neutrons and $a = 0.68$ fm for protons.

The strength of the monopole pairing interaction has been adjusted to reproduce the experimental values of the odd-even mass differences for all considered nuclei.

The quadrupole-quadrupole, octupole-octupole, and hexadecupole-hexadecupole interactions are used below as the residual forces. These factorized multipole-multipole forces are rather schematic. However, these forces are adjusted to selected experimental data. The factorized multipole-multipole interactions have been used in many calculations of the properties of the low–lying collective and two-quasiparticle

TABLE V. Experimental $E^*_{\mathrm{exp}}$ and calculated $E^*_{\mathrm{cal}}$ excitation energies and the structure of the excited states of $^{253}$Es. The energies are given in keV. The experimental data are taken from [32]. $Q_{\lambda\mu}$ denotes a phonon of multipolarity $\lambda\mu$ and $i = 1$.

| $J^\pi$ | $E^*_{\mathrm{exp}}$ | $E^*_{\mathrm{cal}}$ | Structure |
|---|---|---|---|
| $7/2^+$ | 0 | 0 | 7/2[633] 96% |
| $3/2^-$ | 106 | 23 | 3/2[521] 96% |
| $7/2^-$ | 371 | 450 | 7/2[514] 98% |
| $9/2^+$ | | 484 | 9/2[624] 89% + 5/2[512]$\times Q_{32}$ 9% |
| $1/2^-$ | | 562 | 1/2[521] 69% + 3/2[521]$\times Q_{22}$ 29% |
| $5/2^-$ | | 679 | 5/2[512] 71% + 9/2[624]$\times Q_{32}$ 23% |
| $1/2^+$ | | 723 | 1/2[660] 77% + 3/2[651]$\times Q_{22}$ 17% |
| $5/2^-$ | | 735 | 5/2[523] 95% |
| $3/2^+$ | | 801 | 7/2[633]$\times Q_{22}$ 96% |
| $5/2^+$ | | 823 | 5/2[642] 80% + 1/2[530]$\times Q_{32}$ 8% + 5/2[642]$\times Q_{20}$ 6% |
| $7/2^-$ | | 863 | 3/2[521]$\times Q_{22}$ 100% |
| $3/2^+$ | | 892 | 3/2[651] 61 % + 1/2[660]$\times Q_{22}$ 35% |
| $3/2^-$ | | 926 | 7/2[633]$\times Q_{32}$ 97% |
| $1/2^-$ | | 948 | 3/2[521]$\times Q_{22}$ 57% + 1/2[521] 26% + 1/2[530] 12% |
| $1/2^+$ | | 956 | 3/2[521]$\times Q_{32}$ 97% |
| $7/2^+$ | | 987 | 3/2[521]$\times Q_{32}$ 99% |

states performed in the framework of the quasiparticle-phonon model [4, 6, 28]. Thus, these forces have been tested in the known regions of the nuclide chart. Good agreement with the experimental data obtained previously shows that the model can be used to predict the properties of nuclei in the new region. As the result of the previous calculations we know the values of the multipole-multipole interaction constants determined for the rare-earth and actinide regions. At the same time we know from the self-consistent estimations of the interaction constants of the multipole-multipole forces that they are smooth functions of the mass number $A$ [29].

TABLE VI. Experimental $E^*_{\mathrm{exp}}$ and calculated $E^*_{\mathrm{cal}}$ excitation energies and the structure of the excited states of $^{249}$Md. The energies are given in keV. The experimental data are taken from [32]. $Q_{\lambda\mu}$ denotes a phonon of multipolarity $\lambda\mu$ and $i = 1$.

| $J^\pi$ | $E^*_{\mathrm{exp}}$ | $E^*_{\mathrm{cal}}$ | Structure |
|---|---|---|---|
| $9/2^+$ | | 0 | 9/2[624] 90% + 5/2[512]$\times Q_{32}$ 8% |
| $7/2^-$ | 0 | 13 | 7/2[514] 98% |
| $1/2^-$ | | 199 | 1/2[521] 98% |
| $3/2^-$ | | 234 | 3/2[521] 84% + 7/2[633]$\times Q_{32}$ 12% |
| $7/2^+$ | | 249 | 7/2[633] 84% + 3/2[521]$\times Q_{32}$ 12% |
| $5/2^-$ | | 278 | 5/2[512] 74% + 9/2[624]$\times Q_{32}$ 23% |
| $1/2^+$ | | 1022 | 3/2[521]$\times Q_{32}$ 94% |
| $3/2^+$ | | 1036 | 7/2[514]$\times Q_{32}$ 95% |
| $3/2^-$ | | 1109 | 7/2[633]$\times Q_{32}$ 84% + 3/2[521] 12% |
| $7/2^+$ | | 1118 | 7/2[633]$\times Q_{20}$ 57% + 3/2[521]$\times Q_{32}$ 42% |
| $5/2^-$ | | 1174 | 5/2[523] 93% |
| $7/2^-$ | | 1180 | 7/2[514]$\times Q_{20}$ 100% |
| $5/2^+$ | | 1206 | 5/2[642] 59% + 3/2[521]$\times Q_{31}$ 25% |
| $3/2^+$ | | 1212 | 1/2[521]$\times Q_{32}$ 94% |
| $5/2^+$ | | 1221 | 1/2[521]$\times Q_{32}$ 97% |
| $1/2^+$ | | 1279 | 1/2[660] 55% + 3/2[521]$\times Q_{31}$ 33% |
| $9/2^+$ | | 1343 | 9/2[624]$\times Q_{20}$ 100% |
| $1/2^-$ | | 1378 | 1/2[521]$\times Q_{20}$ 100% |

Therefore we can extrapolate the interaction constants from the known regions of $Z$ and $A$ to nuclei with $Z \approx 100$.

Finally, the Hamiltonian (1) is expressed in terms of the quasiparticle creation and annihilation operators obtained from the corresponding particle operators through the $u$-$v$ Bogoliubov transformation. The quasiparticle Hamiltonian is then adopted to solve the random phase approximation (RPA) eigenvalue equations and generates the RPA phonon operators and the quasiparticle-phonon interaction term.

The Hamiltonian expressed in terms of the quasiparticle and phonon creation and annihilation operators has the form

$$H = \sum_q \varepsilon_q \alpha_q^+ \alpha_q + \sum_\nu \hbar\omega_\nu Q_\nu^+ Q_\nu + \sum_{q,q',\nu} f_{qq'}^{(\nu)} \alpha_q^+ \alpha_{q'} (Q_\nu^+ + Q_\nu). \quad (3)$$

Here the operator $\alpha_q^+$ is a quasiparticle creation operator with quantum number $q$, and $\nu$ stands for the phonon quantum number $\nu = \lambda\mu i$, where $i = 1,2,\ldots$ label RPA phonons with given multipolarity $\lambda\mu$ in accordance with the phonon excitation energy; i.e., the one-phonon state $Q^+_{\lambda\mu 1}|0\rangle_{RPA}$ has the lowest energy. The vector $|0\rangle_{RPA}$ is a phonon vacuum state.

This Hamiltonian is diagonalized in a configurational space which includes one-quasiparticle and one-quasiparticle⊗phonon states. Correspondingly, the wave function of the state of the odd-proton nucleus takes the form

$$|\Psi_n\rangle = \left( \sum_q C_q^n \alpha_q^+ + \sum_{q\nu} D_{q\nu}^n \alpha_q^+ Q_\nu^+ \right) |0\rangle_{RPA}. \quad (4)$$

We have taken into account the phonons with the quantum numbers $\lambda\mu = 20$, 22, 30, 31, 32, and 44 and several values of $i$. The single-particle spectrum was taken from the bottom of the mean field potential up to +5 MeV.

TABLE VII. Experimental $E^*_{exp}$ and calculated $E^*_{cal}$ excitation energies and the structure of the excited states of $^{255}$Md. The energies are given in keV. The experimental data are taken from [32]. $Q_{\lambda\mu}$ denotes a phonon of multipolarity $\lambda\mu$ and $i = 1$.

| $J^\pi$ | $E^*_{exp}$ | $E^*_{cal}$ | Structure |
|---|---|---|---|
| $7/2^-$ | 0 | 0 | 7/2[514] 98% |
| $9/2^+$ | | 41 | 9/2[624] 91% + 5/2[512]$\times Q_{32}$ 8% |
| $1/2^-$ | | 211 | 1/2[521] 98% |
| $3/2^-$ | | 261 | 3/2[521] 84% + 7/2[633]$\times Q_{32}$ 12% |
| $7/2^+$ | | 272 | 7/2[633] 85% + 3/2[521]$\times Q_{32}$ 11% |
| $5/2^-$ | | 276 | 5/2[512] 76% + 9/2[624]$\times Q_{32}$ 20% |
| $3/2^-$ | | 794 | 7/2[514]$\times Q_{22}$ 95% |
| $3/2^+$ | | 794 | 7/2[633]$\times Q_{22}$ 96 % |
| $1/2^-$ | | 858 | 3/2[521]$\times Q_{22}$ 98% |
| $7/2^-$ | | 877 | 3/2[521]$\times Q_{22}$ 100% |
| $5/2^+$ | | 990 | 9/2[624]$\times Q_{22}$ 98% |
| $1/2^+$ | | 1046 | 3/2[521]$\times Q_{32}$ 70% + 1/2[660] 21% |
| $3/2^+$ | | 1068 | 3/2[651] 9% + 7/2[514]$\times Q_{32}$ 86% |
| $5/2^-$ | | 1088 | 1/2[521]$\times Q_{22}$ 98% |
| $1/2^+$ | | 1166 | 1/2[660] 49% + 3/2[521]$\times Q_{32}$ 27% + 3/2[651]$\times Q_{22}$ 15% |
| $7/2^+$ | | 1197 | 7/2[633] 8% + 3/2[521]$\times Q_{32}$ 86% |
| $5/2^+$ | | 1271 | 1/2[521]$\times Q_{32}$ 97% |

## III. RESULTS OF CALCULATIONS OF THE EXCITATION ENERGIES AND THE QUASIPARTICLE-PHONON STRUCTURE OF THE LOW-LYING STATES

The results of calculations of the excitation energies and the quasiparticle-phonon structure of the states of the odd-proton nuclei $^{239–251}$Bk, $^{243–255}$Es, $^{247–257}$Md, $^{253,255}$Lr, and $^{261,263}$Db with excitation energies up to 1400 keV are presented in the Tables I–IX and Figs. 1–6. Comparison of the calculated results with the experimental information on the angular momenta and parities of the ground states of the considered nuclei demonstrates a qualitative agreement.

TABLE VIII. Experimental $E^*_{exp}$ and calculated $E^*_{cal}$ excitation energies and the structure of the excited states of $^{253}$Lr. The energies are given in keV. The experimental data are taken from [32]. $Q_{\lambda\mu}$ denotes a phonon of multipolarity $\lambda\mu$ and $i = 1$.

| $J^\pi$ | $E^*_{exp}$ | $E^*_{cal}$ | Structure |
|---|---|---|---|
| $9/2^+$ | | 0 | 9/2[624] 93% |
| $7/2^-$ | 0 | 91 | 7/2[514] 98% |
| $1/2^-$ | | 91 | 1/2[521] 98% |
| $5/2^-$ | | 173 | 5/2[512] 85% + 9/2[624]$\times Q_{32}$ 12% |
| $3/2^-$ | | 626 | 3/2[521] 80% + 7/2[633]$\times Q_{32}$ 16% |
| $7/2^+$ | | 638 | 7/2[633] 81% + 3/2[521]$\times Q_{32}$ 16% |
| $3/2^+$ | | 1082 | 7/2[514]$\times Q_{32}$ 93% |
| $3/2^+$ | | 1183 | 1/2[521]$\times Q_{32}$ 97% |
| $5/2^+$ | | 1195 | 1/2[521]$\times Q_{32}$ 97% |
| $5/2^-$ | | 1245 | 5/2[512] 11% + 9/2[624]$\times Q_{32}$ 82% |
| $1/2^-$ | | 1285 | 1/2[510] 81% + 5/2[512]$\times Q_{22}$ 8% |
| $3/2^-$ | | 1285 | 7/2[514]$\times Q_{22}$ 91% + 3/2[501] 6% |
| $5/2^+$ | | 1374 | 9/2[624]$\times Q_{22}$ 93% |
| $7/2^-$ | | 1398 | 7/2[514]$\times Q_{20}$ 100% |
| $1/2^+$ | | 1430 | 5/2[512]$\times Q_{32}$ 82% + 1/2[660] 10% |
| $9/2^+$ | | 1467 | 9/2[624]$\times Q_{20}$ 100% |
| $1/2^+$ | | 1586 | 1/2[521]$\times Q_{31}$ 92% |

From the experimental data it is known that in the isotopes of Bk the lowest lying $7/2^+$ and $3/2^-$ states are very close in energy. In the majority of the isotopes $3/2^-$ is the ground state. However, in $^{243}$Bk and $^{249}$Bk the ground state is $7/2^+$. Our calculations reproduce a closeness of $7/2^+$ and $3/2^-$ states. In $^{243}$Bk and $^{247–251}$Bk their splitting is equal to 40 keV or even smaller. However, in $^{239}$Bk the excitation energy of the $3/2^-$ state is 166 keV. In all considered isotopes of Bk we obtain $7/2^+$ as the ground state.

In the case of $^{247,249,253,255}$Es the results of calculations show that the ground state is $7/2^+$, in agreement with the experimental data. The calculations reproduce the closeness in energy of the $7/2^+$ and $3/2^-$ states, in agreement with the experimental data.

In the case of Md isotopes the experimental data indicate the $7/2^-$ state as the ground state. In $^{251–257}$Md the calculated ground state is also $7/2^-$. The calculations show that near the ground state is located the $9/2^+$ level.

The results of calculations for $^{253,255}$Lr show that the ground state is $9/2^+$. However, two closely lying states $7/2^-$ and $1/2^-$ have excitation energies around 90 keV. In the case of $^{261,263}$Db two excited levels $1/2^-$ and $9/2^+$ have practically coinciding excitation energies. Their splitting is less than 20 keV. The calculated ground state is $5/2^-$.

As is seen from the results presented in the tables, all states discussed above lying near the ground state are the one-quasiparticle states. Practically in all cases a contribution of the one-quasiparticle component into the quasiparticle-phonon structure of these states is larger than 90%. However, in $^{239}$Bk the calculated contribution of the one-quasiparticle component 7/2[633] into the structure of the ground states is 79%.

Thus the quasiparticle-phonon structure of the calculated states located below 400 keV shows that these states are of the one-quasiparticle type, with the contribution of the one-quasiparticle component into the structure of these states exceeding 70%. However, in the interval 400–600 keV of the

TABLE IX. Calculated $E^*_{\rm cal}$ excitation energies and the structure of the excited states of $^{263}$Db. The energies are given in keV. $Q_{\lambda\mu}$ denotes a phonon of multipolarity $\lambda\mu$ and $i = 1$.

| $J^\pi$ | $E^*_{\rm cal}$ | Structure |
|---|---|---|
| $5/2^-$ | 0 | 5/2[512] 91% |
| $1/2^-$ | 93 | 1/2[521] 94% |
| $9/2^+$ | 105 | 9/2[624] 95% |
| $7/2^-$ | 258 | 7/2[514] 97% |
| $3/2^-$ | 623 | $1/2[521]\times Q_{22}$ 48% + 3/2[521] 38% + $7/2[633]\times Q_{32}$ 6% |
| $1/2^-$ | 631 | $5/2[512]\times Q_{22}$ 59% + 1/2[501] 14% + 1/2[510] 13% + $5/2[512]\times Q_{22}$ 10% |
| $5/2^+$ | 745 | $9/2[624]\times Q_{22}$ 94% |
| $3/2^-$ | 764 | $7/2[514]\times Q_{22}$ 87% + 3/2[501] 8% |
| $5/2^-$ | 768 | $1/2[521]\times Q_{22}$ 94% |
| $7/2^+$ | 876 | 7/2[633] 76% + $3/2[521]\times Q_{32}$ 19% |
| $9/2^-$ | 902 | $5/2[512]\times Q_{22}$ 99% |
| $3/2^+$ | 1001 | $7/2[514]\times Q_{32}$ 86% + 3/2[651] 6% |
| $5/2^+$ | 1011 | $5/2[624]\times Q_{22}$ 92% |
| $7/2^-$ | 1016 | 7/2[503] 54% + $11/2[615]\times Q_{32}$ 38% |
| $3/2^+$ | 1020 | $1/2[521]\times Q_{32}$ 92% |
| $1/2^+$ | 1098 | $5/2[512]\times Q_{32}$ 89% + 1/2[660] 6% |
| $9/2^-$ | 1141 | $5/2[512]\times Q_{22}$ 98% |

excitation energies, there appear in $^{239}$Bk, $^{255}$Es, and $^{263}$Db states of mixed structure; i.e., the wave functions of these states contain no components whose weight exceeds 70%. In $^{257}$Md and $^{261}$Db in this interval of the excitation energies there appear states whose wave functions contain a significant amount of the one-quasiparticle⊗phonon component. States with a large amount, i.e., exceeding 70%, of the one-quasiparticle⊗phonon component appear above 800 keV.

Very interesting excitation spectra are obtained for the $^{247–253}$Md isotopes. The calculated spectra show a large gap, of the order of 800 keV, between the five low-lying one-quasiparticle states and the the one-quasiparticle⊗phonon excitations. A similar picture is obtained also for $^{253,255}$Lr. In these nuclei there are three closely lying one-quasiparticle states near the ground state. Around 550 keV there are two closely lying one-quasiparticle states $7/2^+[633]$ and $3/2^-[521]$, and the states with mainly phonon components appear above 1 MeV.

Let us discuss the variations of the excitation spectra with the proton number in more detail. At the deformation $\beta_2 = 0.26$ the proton Fermi level lies in Bk and Es isotopes very close to the single-particle levels $7/2^+[633]$ and $3/2^-[521]$. The splitting of these two levels is very small. As a result, practically in all Bk isotopes the first excited state is very close to the ground state. In $^{243,247–251}$Bk this splitting is equal to 10–30 keV. In the single-particle scheme the levels $1/2^+[660]$, $5/2^-[523]$ and $3/2^-[521]$ are located below $7/2^+[633]$ and $3/2^-[521]$ levels. The excited states whose structure is mainly exhausted by one of the one-quasiparticle components $1/2^+[660]$, $5/2^-[523]$, and $3/2^-[521]$ appear at excitation energies of 400–600 keV. The excited states whose main component is quasiparticle⊗phonon appear at excitation energies around 1 MeV. However, in $^{251}$Bk one state with a large weight of such a component has an excitation energy ∼600 keV. The reason for the lowering of its excitation energy is a strong decrease of the energy of the $\gamma$ phonon ($K^\pi = 2^+$) when the number of neutrons approaches $N = 156$. This effect is discussed in [30] and is explained by the fact that at $N = 156$ the neutron Fermi level is located just between single-particle levels belonging to the weakly split pseudospin doublet $3/2^+[622]$, 1/2+[620]. The corresponding two-quasiparticle state can have $K^\pi = 2^+$. A similar picture is observed in Es isotopes since in Es and Bk the last protons occupy one of the closely lying single-particle levels. Due to the same reason as in Bk isotopes, the states with a large weight of the one-quasiparticle⊗$\gamma$-phonon component decrease in excitation energy up to 500–600 keV in the isotopes $^{253}$Es ($N = 154$) and $^{255}$Es ($N = 156$).

Consider now Md isotopes. In Es isotopes the proton Fermi level lies close to the single-particle levels $7/2^+[633]$, $3/2^-[521]$ and is separated significantly from the single-particle levels $9/2^+[624]$, $7/2^-[514]$. In contrast to this, in Md isotopes the proton Fermi level lies approximately between the two groups of the single-particle levels mentioned above. As a result, in Es isotopes excited states with a large weight of the one-quasiparticle component $9/2^+[624]$ or $7/2^-[514]$ have excitation energies around 500 keV. However, in Md isotopes the distance between the two groups of states—the lower of which is based on the $9/2^+[624]$, $7/2^-[514]$ one-quasiparticle states and the higher one is based on the $7/2^+[633]$, $3/2^-[521]$ one-quasiparticle states—decreases up to 200-300 keV. In addition, the single-particle levels $1/2^-[521]$ and $5/2^-[512]$ become closer to the Fermi level and the corresponding one-quasiparticle energies also decrease. As a result of this decrease of the excitation energies of the states having mainly the one-quasiparticle structure, a gap of the order of 700–800 keV appears in the excitation spectra of the Md isotopes. In the case of the Es and Md isotopes the energies of the phonon excitations are of the order of 1 MeV.

An increase of the number of protons in Lr compared to Md leads to even larger separation of the single-particle levels $7/2^+[633]$ and $3/2^-[521]$ from the Fermi level. As

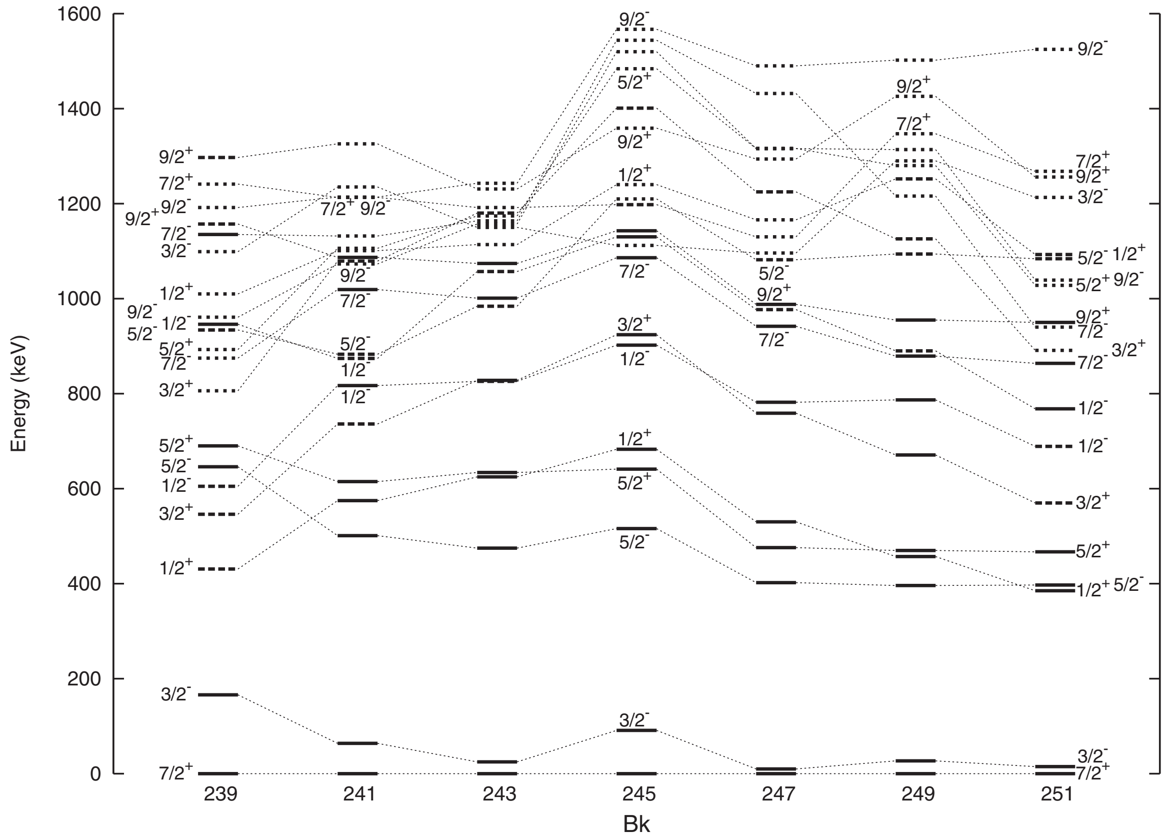


FIG. 1. The calculated spectra of the low-lying excited states of the odd isotopes of Bk. The solid lines denote states with the one-quasiparticle component contributing more than 70% of the norm. The dotted lines correspond to the states with the contribution of the quasiparticle⊗phonon component exceeding 70%. Other states are denoted by the dashed lines.

a result, the excitation energies of the states, whose structure is determined by the corresponding one-quasiparticle components, increase and in the calculated spectra of Lr isotopes there appear two states with an excitation energy ∼600 keV. The excitations whose structure is characterized by the one-quasiparticle⊗phonon component lie in Lr isotopes above 1 MeV as in the case of Md isotopes. Since in $^{253,255}$Lr the numbers of neutrons are removed from $N = 156$, the energies of the $\gamma$-vibrational phonons are high.

The isotopic dependence of the excitation spectra is illustrated by Figs. 1–4. The structure of the spectra near the ground state is rather stable with respect to variation of the number of neutrons. For instance, the excitation energy of the $7/2^-$ state in the isotopes of Es located around 500 keV varies very little with the number of neutrons. This result is in contradiction, however, with the experimental results of [31]. The energies of some of the higher excitation states vary significantly with the variation of the number of neutrons.

It was mentioned in Sec. II that the results of several calculations demonstrate a stability of the equilibrium quadrupole deformation of nuclei with $Z = 100$–104. The results presented in Fig. 5 for $^{243}$Es show that the excitation spectrum of this nucleus do not change significantly if $\beta_2$ varies from 0.22 to 0.28. However, when $\beta_2$ takes the value 0.30 the excitation spectrum changes significantly. It happens because two single-particle levels $1/2^+[660]$ and $3/2^+[651]$ whose energies increase very strongly with deformation become very close to $3/2^-[521]$ and $7/2^+[633]$ at $\beta_2 = 0.30$. As a result the excitation spectrum of $^{243}$Es changes significantly compared to that at smaller deformations. The excitation energies and the structure of the states of $^{243}$Es at $\beta_2 = 0.30$ are presented in Table X.

The effect of blocking of the single-particle states by the odd proton and the effect of the quasiparticle-phonon interaction on the excitation spectra is illustrated by Fig. 6 for $^{249}$Bk. It is seen from this figure that, although the ground and the first excited state are very close in energy in all cases shown in Fig. 6 (only ordering of the $7/2^+$ and $3/2^-$ states can be changed), the excitation energies of the other states change significantly depending on what effects are taken into account in the calculations.

It is interesting to mention that the inclusion in the calculations of the blocking effect changes significantly the results obtained in the BCS approximation. However, the quasiparticle-phonon coupling, taken into account together with the blocking effect, gives final results somewhat closer to those obtained in the BCS approximation.

Let us compare the results of our calculations with those presented in [1] and [2]. In these papers the quasiparticle-phonon coupling was not taken into account, in contrast to our calculations. However, in these calculations as in ours the Woods-Saxon potential was used as an approximation to the nuclear mean field, but with different parameters.

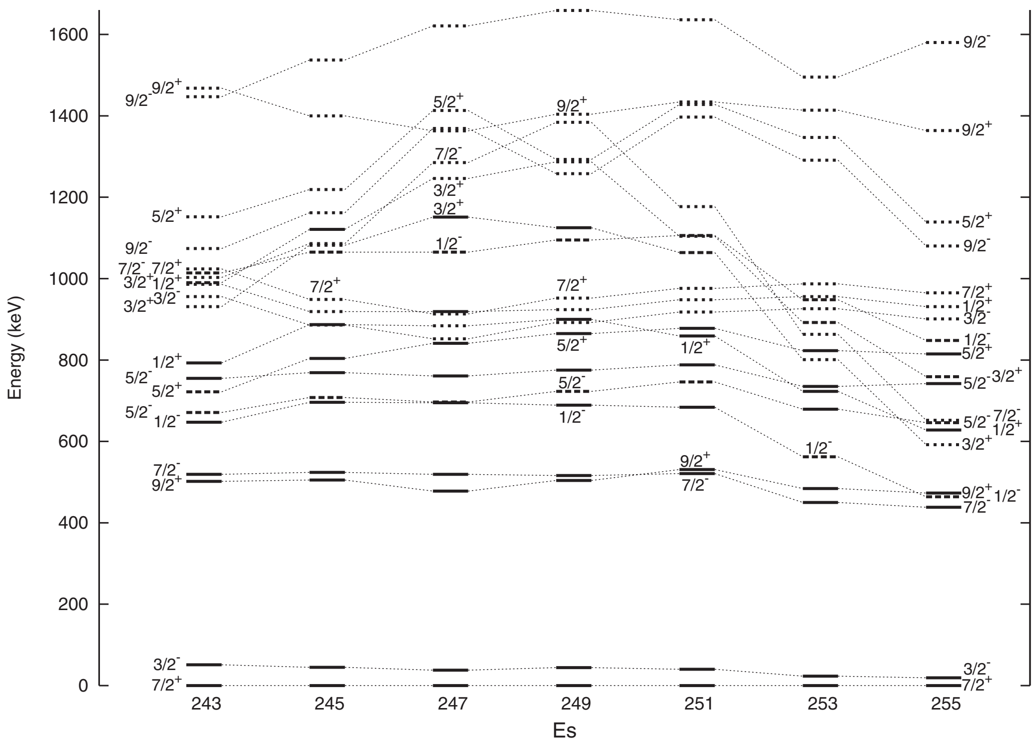


FIG. 2. The calculated spectra of the low-lying excited states of the odd isotopes of Es. Solid lines denote the states with the one-quasiparticle component contributing more than 70% of the norm. The dotted lines correspond to the states with the contribution of the quasiparticle⊗phonon component exceeding 70%. Other states are denoted by the dashed lines.

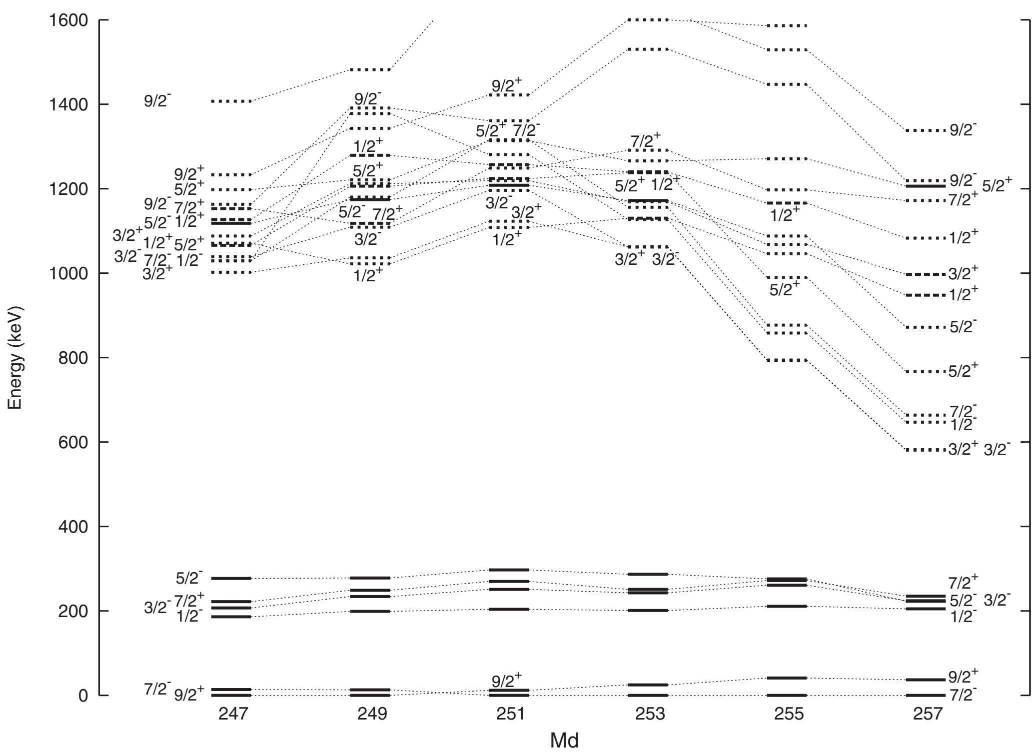


FIG. 3. The calculated spectra of the low-lying excited states of the odd isotopes of Md. The solid lines denote the states with the one-quasiparticle component contributing more than 70% of the norm. The dotted lines correspond to the states with the contribution of the quasiparticle⊗phonon component exceeding 70%. Other states are denoted by the dashed lines.

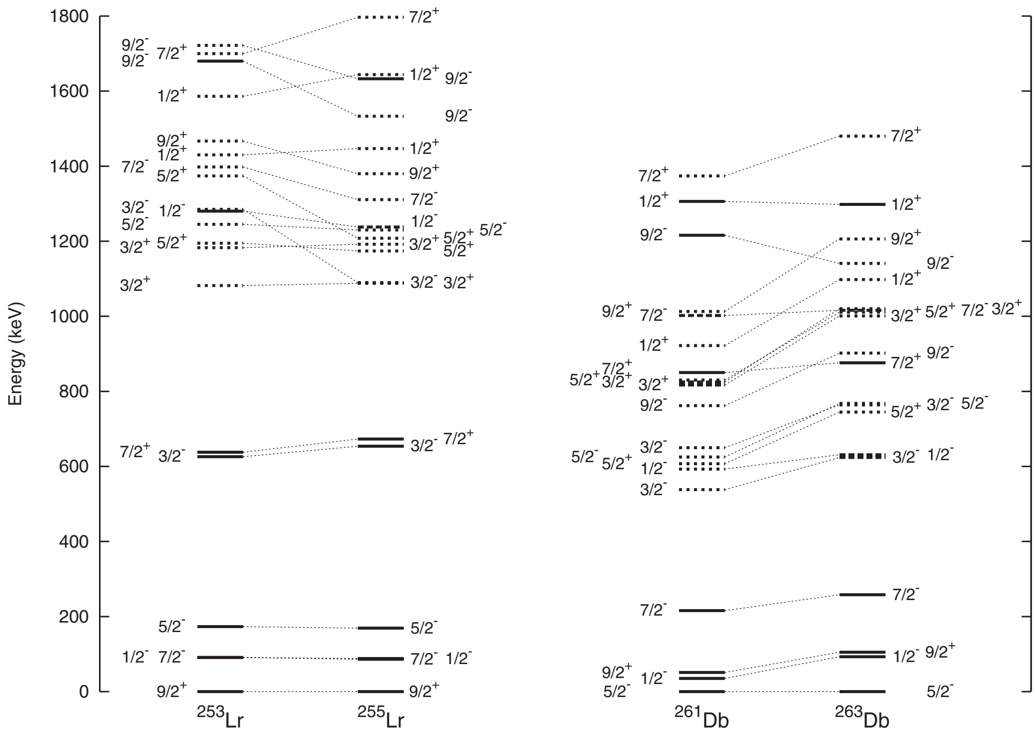


FIG. 4. The calculated spectra of the low-lying excited states of the odd isotopes of Lr and Db. The solid lines denote the states with the one-quasiparticle component contributing more than 70% of the norm. The dotted lines correspond to the states with the contribution of the quasiparticle⊗phonon component exceeding 70%. Other states are denoted by the dashed lines.

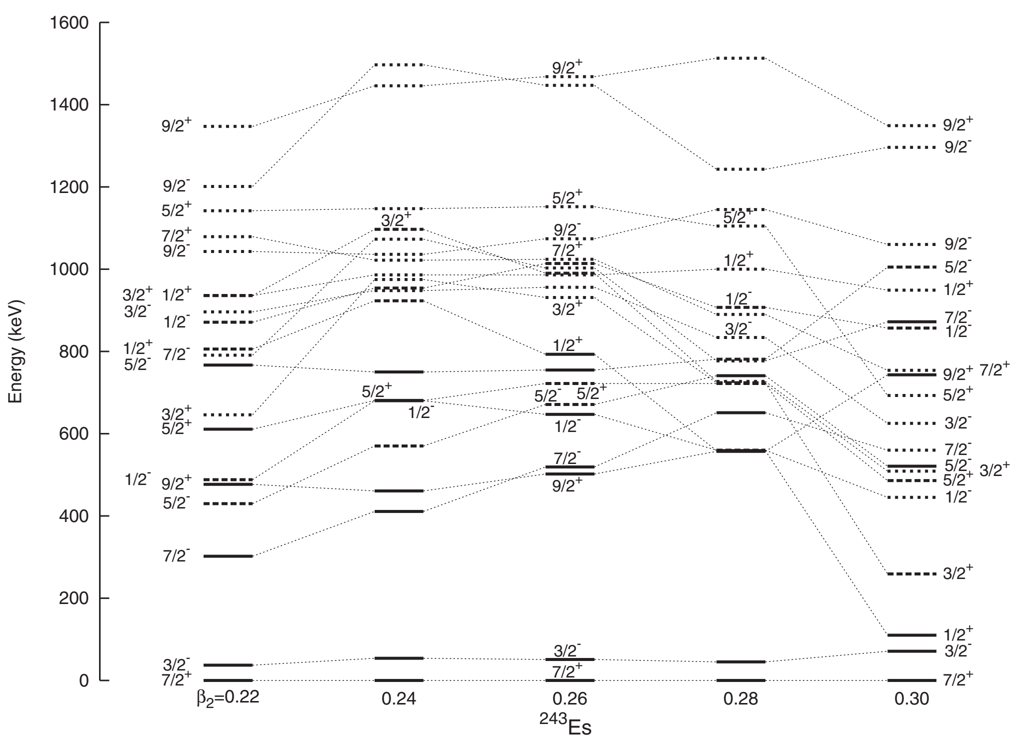


FIG. 5. Dependence of the spectra of the low-lying excited states of $^{243}$Es on the value of the quadrupole deformation. The solid lines denote the states with the one-quasiparticle component contributing more than 70% of the norm. The dotted lines correspond to the states with the contribution of the quasiparticle⊗phonon component exceeding 70%. Other states are denoted by the dashed lines.

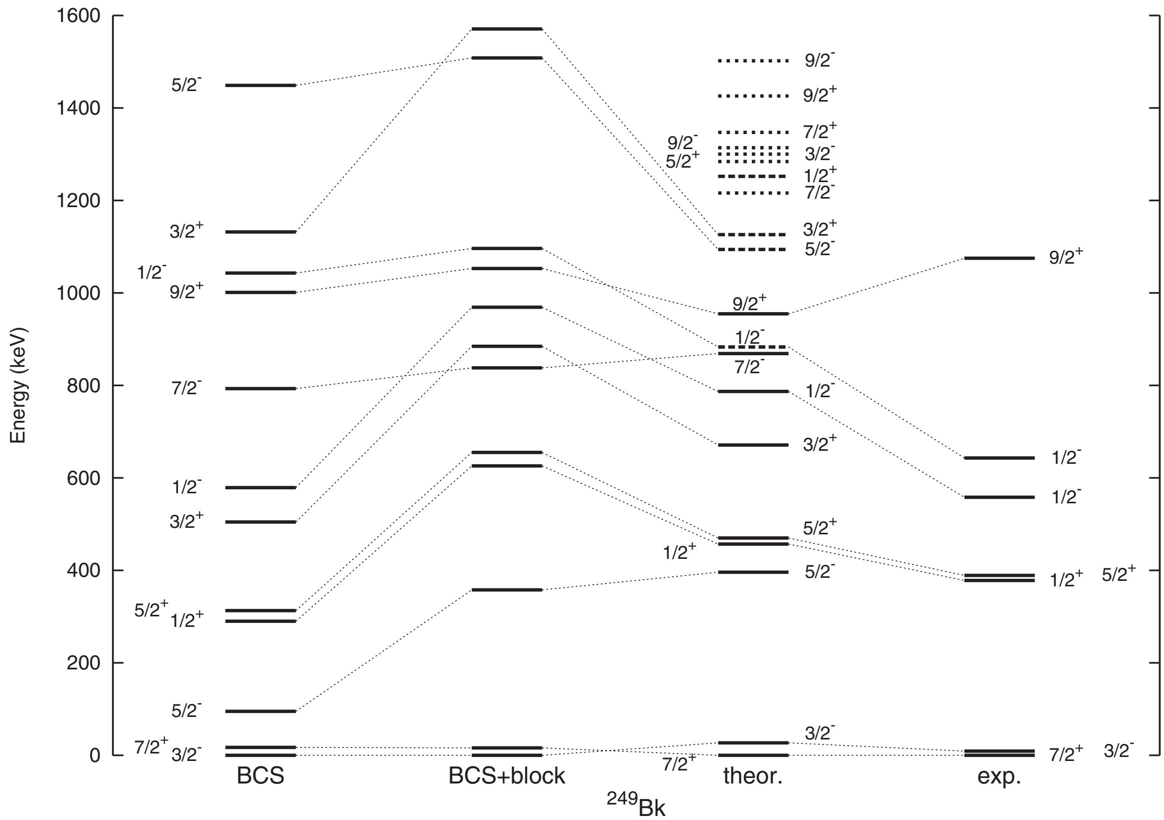


FIG. 6. The results of calculation of the spectra of the low-lying excited states of $^{249}$Bk in different approximations. BCS: BCS approximation without blocking and the quasiparticle-phonon interaction; BCS+block: BCS approximation plus blocking effect; theor.: BCS approximation plus blocking effect plus quasiparticle-phonon interaction. The solid lines denote the states with the one-quasiparticle component contributing more than 70% of the norm. The dotted lines correspond to the states with the contribution of the quasiparticle⊗phonon component exceeding 70%. Other states are denoted by the dashed lines.

TABLE X. Calculated $E^*_{\rm cal}$ excitation energies and the structure of the excited states of $^{243}$Es for $\beta_2 = 0.30$. The energies are given in keV. $Q_{\lambda\mu}$ denotes a phonon of multipolarity $\lambda\mu$ and $i = 1$.

| $J^\pi$ | $E^*_{\rm cal}$ | Structure |
|---|---|---|
| $7/2^+$ | 0 | $7/2[633]$ 78% + $7/2[633]\times Q_{20}$ 19% |
| $3/2^-$ | 71 | $3/2[521]$ 89% |
| $1/2^+$ | 110 | $1/2[660]$ 72% + $3/2[651]\times Q_{22}$ 15% + $1/2[660]\times Q_{20}$ 8% |
| $3/2^+$ | 259 | $3/2[651]$ 61% + $1/2[660]\times Q_{22}$ 32% |
| $1/2^-$ | 445 | $3/2[521]\times Q_{22}$ 75% + $1/2[521]$ 22% |
| $5/2^+$ | 486 | $5/2[642]$ 63% + $5/2[642]\times Q_{20}$ 31% |
| $3/2^+$ | 509 | $7/2[633]\times Q_{22}$ 95% |
| $5/2^-$ | 511 | $5/2[523]$ 78% + $5/2[523]\times Q_{20}$ 20% |
| $7/2^-$ | 560 | $3/2[521]\times Q_{22}$ 100% |
| $3/2^-$ | 625 | $3/2[521]\ \times Q_{20}$ 94% |
| $5/2^+$ | 693 | $1/2[660]\times Q_{22}$ 89% + $5/2[402]$ 10% |
| $9/2^+$ | 743 | $9/2[624]$ 90% |
| $7/2^+$ | 744 | $7/2[633]\times Q_{20}$ 81% + $7/2[633]$ 18% |
| $1/2^-$ | 857 | $1/2[521]$ 64% + $3/2[521]\times Q_{22}$ 19% + $1/2[521]\times Q_{20}$ 9% |
| $7/2^-$ | 872 | $7/2[514]$ 97% |
| $1/2^+$ | 949 | $1/2[660]\times Q_{20}$ 83% + $3/2[651]\times Q_{22}$ 16% |
| $5/2^-$ | 1004 | $5/2[512]$ 58% + $9/2[624]\times Q_{32}$ 14% + $7/2[633]\times Q_{31}$ 13% + $1/2[521]\times Q_{202}$ 9% |
| $9/2^-$ | 1060 | $5/2[523]\times Q_{22}$ 100% |
| $9/2^-$ | 1296 | $7/2[633]\times Q_{31}$ 98% |
| $9/2^+$ | 1349 | $9/2[624]\times Q_{20}$ 98% |

Consider as an example the excitation spectra of Bk isotopes. In all the calculations the lowest-lying states are $7/2^+$ and $3/2^-$. However, a splitting of these states is much smaller in our calculations than in [1, 2]. Our results are in agreement with the experimental data. There are also some differences in the energies of the other states. At the same time in some nuclei the calculated spectra have a similar structure. For instance, in $^{249,251}$Bk in our calculations as in the calculations performed in [1] and [2] the excited states just above the ground state are $1/2^+$ and $5/2^+$. However, in our calculations near these states there is the $5/2^-$ state with a large contribution of the one-quasiparticle component.

In our calculations, as in the calculations performed in [1], in the Es isotopes the lowest four levels are $7/2^+$, $3/2^-$, $7/2^-$, and $1/2^-$. However, again in our calculations the ground states and the first excited state are much closer in energy than in the calculations of [1]. Additionally in our calculations the $9/2^+$ state having mainly the one-quasiparticle structure appears close to $7/2^-$ and $1/2^-$ states .

In the calculations of [1] performed for $^{253,255}$Es the first excited state is $1/2^-$, in contrast to our results.

In our calculations performed for the Md isotopes the $9/2^+$ state appears very close to the ground state or as the ground state. In the calculations of [1] and [2] the $9/2^+$ state has a larger excitation energy. As the ground state of $^{251,253,255,257}$Md we obtain the $7/2^-$ state. The calculations of [1] and [2] predict $1/2^-$ as the ground state.

For $^{253,255}$Lr our calculations, as the calculations of [1] and [2], predict that the lower-lying states are $9/2^+$, $7/2^-$, and $1/2^-$. In the case of $^{261,263}$Db all these calculations predict that the ground state is $9/2^+$. Our calculations predict also an appearance of the $1/2^-$ state near the ground state. Calculations of [1] and [2] predict for this state an excitation energy around 300 keV.

## IV. SUMMARY

In summary, we have presented the results of calculations of the excitation energies and the structure of the low-lying states of the odd-$Z$ nuclei with $Z \approx 100$. The quasiparticle-phonon interaction and the blocking effect have been taken into account in the calculations. It is shown that below 400 keV the main component in the structure of the states is a one-quasiparticle component. However, above 600 keV the excitation of the phonons and the quasiparticle-phonon interaction begin to play an important role in a description of the properties of the excited states of nuclei with $Z \approx 100$.

## ACKNOWLEDGMENTS

The authors are grateful to Professor N. V. Antonenko, Professor P. von Brentano, and Professor L. A. Malov for the useful discussions. This work was supported by the RFBR (Russia) under Grant No. 10-02-00301, by the DFG (Germany) under Contract No. Br 799/25-1, and by the Heisenberg-Landau Program.

[1] S. Cwiok, S. Hofmann, and W. Nazarewicz, Nucl. Phys. A **573**, 356 (1994).
[2] A. Parhomenko and A. Sobiczewski, Acta. Phys. Pol. **35**, 2447 (2004).
[3] E. Litvinova, Phys. Rev. C **85**, 021303 (2012).
[4] V. G. Soloviev, *Theory of Atomic Nuclei: Quasiparticles and Phonons* (Institute of Physics, Bristol, 1992).
[5] S. P. Ivanova, A. L. Komov, L. A. Malov, Phys. Part. Nucl. **7**, 450 (1976).
[6] V. G. Soloviev, A. V. Sushkov, N. Yu. Shirikova, Phys. Part. Nucl. **27**, 667 (1996).
[7] V. G. Soloviev, A. V. Sushkov, N. Yu. Shirikova, N. Lo Iudice, Nucl. Phys. A **613**, 45 (1997).
[8] M. Bender, P.-H. Heenen, and P.-G. Reinhardt, Rev. Mod. Phys. **75**, 121 (2003).
[9] H. Kucharek and P. Ring, Z. Phys. A **339**, 23 (1991).
[10] H. Lenske and Ch. Fuchs, Phys. Lett. B **345**, 355 (1995).
[11] M. Kortelainen, T. Lesinski, J. More, W. Nazarewicz, J. Sarich N. Schunck M. V. Stoitsov, and S. Wild, Phys. Rev. C **82**, 024313 (2010).
[12] R.-D. Herzberg and P. T. Greenlees, Prog. Part. Nucl. Phys. **61**, 674 (2008).
[13] I. Ahmad, Phys. Scr. T **125**, 78 (2006).
[14] I. Ahmad and R. R. Chasman, Phys. Rev. C **80**, 064315 (2009).
[15] A. V. Afanasjev and S. Frauendorf, Phys. Rev. C **71**, 024308 (2005).
[16] J. C. Pei, F. R. Xu, and P. D. Stevenson, Phys. Rev. C **71**, 034302 (2005).
[17] A. V. Afanasjev, Phys. Scr. T **125**, 62 (2006).
[18] S. Cwiok, J. Dobaczewski, P.-H. Heenen, P. Magiersk, and W. Nazarewicz, Nucl. Phys. A **611**, 211 (1996).
[19] A. Chatillon *et al.*, Eur. Phys. J. A **30**, 397 (2006).
[20] S. Ketelhut *et al.*, Phys. Rev. Lett. **102**, 212501 (2009).
[21] I. Ahmad, Nucl. Radiochem. Sci. **3**, 179 (2002).
[22] I. Ahmad *et al.*, Phys. Rev. C **62**, 064302 (2000).
[23] L. Grodzins, Phys. Lett. **2**, 88 (1962).
[24] P. Reiter *et al.*, Phys. Rev. Lett. **82**, 509 (1999).
[25] S. Cwiok, P.-H. Heenen, and W. Nazarewicz, Nature (London) **433**, 705 (2005).
[26] S. K. Patra, W. Greiner, and R. K. Gupta, J. Phys. G: Nucl. Part. Phys. **26**, L65 (2000).
[27] R. R. Chasman and I. Ahmad, Phys. Lett. B **392**, 255 (1997).
[28] V. G. Soloviev, A. V. Sushkov, N. Yu. Shirikova, Phys. Part. Nucl. **25**, 157 (1994).
[29] A. Bohr and B. Mottelson, *Nuclear Structure*, Vol. 2. (Benjamin, New York, 1975).
[30] R. V. Jolos, N. Yu. Shirikova, and A. V. Sushkov, Phys. Rev. C **86**, 044320 (2012).
[31] F. P. Hessberger *et al.*, Eur. Phys. J. A **26**, 233 (2005).
[32] http://www.nndc.bnl.gov/nndc/ensdf/